Available online at www.sciencedirect.com
ScienceDirect
Sensors and Actuators A 133 (2007) 486–492
SENSORS AND ACTUATORS A PHYSICAL
www.elsevier.com/locate/sna

Theoretical performance of a coiled coil piezoelectric bimorph

K.A. Seffen *

Department of Engineering, University of Cambridge, Trumpington Street, Cambridge CB2 1PZ, United Kingdom

Received 25 October 2005; received in revised form 7 April 2006; accepted 17 April 2006
Available online 23 May 2006

Abstract

The electromechanical coupling behaviour of a novel, highly coiled piezoelectric strip structure is developed in full, in order to expound its performance and efficiency. The strip is doubly coiled for compactness and, compared to a standard straight actuator of the same cross-section, it is shown that the actuator here offers better generative forces and energy conversion, and substantial actuated displacements, however, at the expense of a much lower stiffness. The device is therefore proposed for high-displacement, quasi-static applications.

Keywords: Coiled coil; Piezoelectric; Bimorph; Electromechanical coupling; Efficiency

1. Introduction

Piezoelectric ceramics, such as lead zirconium titanate, or PZT, are well known for their actuation and sensing properties, as found in "smart" transducers where devices can actively respond to, and correct for, potentially damaging loads. This dual functionality derives from the electromechanical coupling behaviour of piezoelectric, which can be expressed in terms of universal material parameters [1] or coefficients pertaining to the shape of a specific device [2]. The latter are especially useful, for they enable transparent measures of transducer efficiency and performance [3] but studies have been confined to prismatic shapes commensurable with commercially available structures. Recent advances in ceramics processing has, however, enabled the means to produce a diversity of shapes [4], in particular, initially *coiled strips*, expeditious in the amplification of naturally small activation strains. Solutions include spirals and helices [5,6], and elegant super-helical forms [7] where the strip follows a doubly curved tortuous path described eponymously as a *coiled coil*. The strip is coiled locally around a larger curved path, which is flat in the case of a toroidal coiled coil or is helical in the case of multiple turns, as reproduced from [7] in Fig. 1(a) and (b), respectively. During activation, the degree of coiling increases, and magnifies displacements along the axis of curving of the larger path up to 25% of its radius for *each turn* of path, according to the provisional assessment in [7]. Within the realm of solid-state actuation, these displacements are significant but they must be set against wider mechanical and electrical performance ranges, and demands an exposition of the full coupling behaviour. Its development is carried out here and is underpinned, first, by a review of the application of piezoelectric material to strip-like structures. Although developed for initially straight strips, the process is extended to coiled structures under key assumptions, which are discussed in detail. Previously defined performance measures are used to characterise the efficiency of the coiled coil, and results are compared to a straight cantilever strip, for extra clarity. The overall effort is entirely theoretical and is intended to complement the design of future actuators; but it is also timely in light of the very recent discovery of *nano-scale* piezoelectric helices [8], and the methods presented here may enable the inventors to quantify their performance – as they propose – as nano-scale actuators and sensors.

2. Coiled bimorph strip behaviour

Consider the straight structure in Fig. 2(a) with two equal layers of piezoelectric material, each with top and bottom electrode surfaces of negligible thickness, but each sharing a central electrode. The piezoelectric layers, of thickness t, are thin compared to their width, w, and narrow compared to their length, L, and it is argued [1] that their constitutive response is adequately

* Tel.: +44 1223 764137; fax: +44 1223 332662.
E-mail address: kas14@cam.ac.uk.

0924-4247/$ – see front matter © 2006 Elsevier B.V. All rights reserved.
doi:10.1016/j.sna.2006.04.016

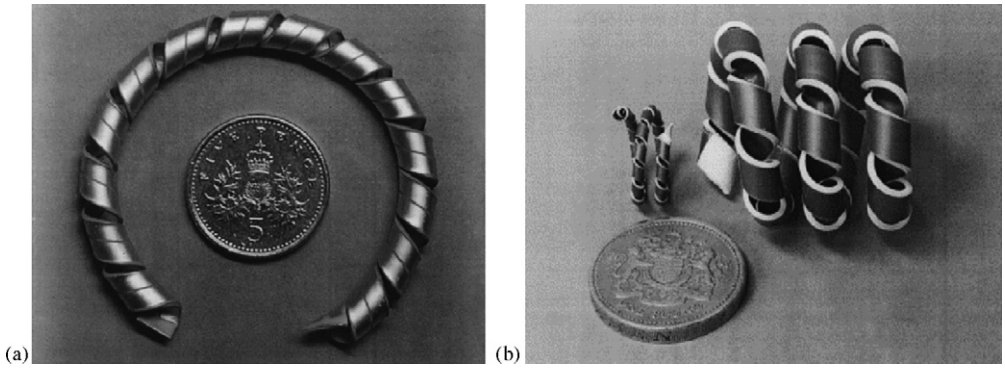

Fig. 1. Types of super-helix, or "coiled coil", reproduced from [7] whose size can be compared to British coins: (a) a flat toroidal coiled coil; (b) two coiled coils of different sizes and multiple turns.

described by a pair of relationships in terms of axial parameters alone:

$$\epsilon = s_{11}^{E}\sigma + d_{31}E_3, \tag{1a}$$

$$D = d_{31}\sigma + e_{33}^{T}E_3. \tag{1b}$$

The symbols ϵ and σ refer to normal strain and stress where elongation and tension are positive quantities. The elastic compliance is s_{11}^{E} but under "short circuit" conditions, as if the top and bottom electrodes in each strip were connected to each other by a length of wire. Activation is wrought by application of an electric field, E_3, via the electrodes in the through thickness, or "3", direction, and the piezoelectric charge constant, d_{31}, refers to its effect in the axial, or "1", direction. The electric "displacement", D, is used to find the total charge stored in the strip and e_{33}^{T} is the dielectric constant under zero stress. Other activation modes are possible, but only under different electrode lay-ups, and are excluded from study here.

During activation, independent electric fields give rise to separate controllable expansions of each layer, and is known familiarly as a *bimorph* operation: a continuity of strains across the overall depth causes bending or stretching or both. As in [7], the layers endure opposing electric fields to maximise the degree of bending and, in Fig. 2(a), the central electrode is set to V volts whilst the outer potentials are set to be the same – usually zero for safety, assuming that the directions of material polarisation in both layers are the same. Actuated displacements therefore derive from the aggregation of bending strains and, thus, a formalised *structural* response of the strip with both layers considers equal and opposite moments, M, applied to the ends of strip, which foist a uniform change in curvature, κ, of its mid-plane, as shown in Fig. 2(b). The integral effect of the parameters in Eqs. (1a) and (1b) can now be computed, specifically, for any axial fibre at a general height, z, above the mid-plane, the strain is $z\kappa$ and, from Eq. (1a), the bending stress resultant is found by integrating the turning effect of σ across both layers, accounting for the correct direction of electric field, and is set equal to M. The final compact expression is

$$\kappa = \frac{12s_{11}^{E}M}{wt^3} + \frac{3d_{31}E_3}{t}, \tag{2}$$

and is the *generalised Hooke's law* for bending of a bimorph strip, for it governs the behaviour under any loads whereby M and κ are the local values of bending moment and curvature. Note that, when no moment is applied, a positive electric field induces positive curvature.

In order to determine the commensurate electrical response, it is usual to assume that D in Eq. (1b) is uniform across the width for a single thin layer, and the charge per unit length, q, can be found from [9]:

$$q = \frac{w}{h/2}\int_0^{t/2} D\,\mathrm{d}z. \tag{3}$$

This calculation is performed by first re-arranging Eq. (1a) and substituting $z\kappa$ for ϵ, with κ from Eq. (2), to give:

$$\sigma = \frac{12Mz}{wt^3} + \frac{d_{31}E_3}{s_{11}^{E}}\left[\frac{3z}{t} - 1\right], \tag{4}$$

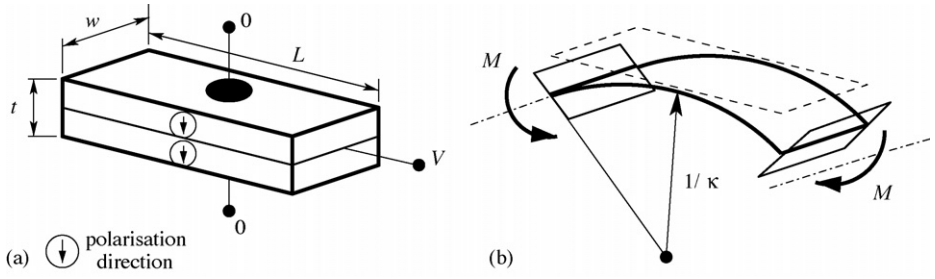

Fig. 2. Operation of an initially straight piezoelectric bimorph strip: (a) geometry, material polarisation and electrical activation. There are two equal thickness strips separated by an electrode at potential V, with two outer surface electrodes held at zero volts; (b) deformed mid-plane surface of strip with uniform curvature, κ; all cross-sections carry the same bending moment, M, but only the two end sections are shown for clarity.

which is then inserted into Eq. (1b):

$$D = d_{31}\frac{12Mz}{wt^3} + e_{33}^T E_3\left[1 - k_{31}^2\left(1 - \frac{3z}{t}\right)\right], \tag{5}$$

where k_{31}^2 has replaced $d_{31}^2/s_{11}^E e_{33}^T$. Eq. (5) is substituted for D in Eq. (3) and integrated over the depth of a single layer for q in terms of M and E_3, which is then doubled for a bimorph, to reveal:

$$q = \frac{6d_{31}M}{t^2} + 2we_{33}^T E_3\left[1 - \frac{k_{31}^2}{4}\right]. \tag{6}$$

Finally, for compactness, Eqs. (2) and (6) can be re-cast as the following matrix equation:

$$\begin{bmatrix}\kappa\\ q\end{bmatrix} = \begin{bmatrix}12s_{11}^E/wt^3 & 3d_{31}/t\\ 6d_{31}/t^2 & 2we_{33}^T[1-(k_{31}^2/4)]\end{bmatrix}\begin{bmatrix}M\\ E_3\end{bmatrix}. \tag{7}$$

Note that the matrix elements do not depend on length, so that κ, M, q and E_3 can be described uniquely along the strip for non-uniform load cases. For example, for a bimorph cantilever built-in at the root and loaded at its tip by a vertical force, F, the bending moment, $M(x)$, at a distance, x, from the root is $F(L-x)$, and the change in curvature is approximately the double derivative of transverse displacements with respect to x. Substituting into the first line of Eq. (7) and integrating twice under the proper boundary conditions at the root produces a general displacement–force–field relationship, which can be specified, say, in terms of the tip displacement, δ, for it characterises the mechanical output of the transducer; in addition, the total charge, Q, can be found by a similar process of integration, the electric field is written via the actual potential difference across each layer from $V = E_3 t/2$, and the matrix above can be commuted to a more definite form:

$$\begin{bmatrix}\delta\\ Q\end{bmatrix} = \begin{bmatrix}A & B\\ B & C\end{bmatrix}\begin{bmatrix}F\\ V\end{bmatrix}, \tag{8}$$

in which:

$$A = \frac{4s_{11}^E}{w}\left(\frac{L}{t}\right)^3, \qquad B = 3d_{31}\left(\frac{L}{t}\right)^2,$$

$$C = 4we_{33}^T\left[1 - \frac{k_{31}^2}{4}\right]\left(\frac{L}{t}\right). \tag{9}$$

Coefficients similar to the above are obtained in [2] where the differences are due to the definition of voltage potential. Other load responses are also divined, but the explicit form described by Eq. (7) is most instrumental in elucidating the coiled coil response. First, careful consideration is paid to its geometry, which is displayed schematically in Fig. 3.

The strip clearly coils in a localised manner, forming a helical path that wraps up into another helix. As in practical structures, both helices are shown as being right-handed throughout, but left-handedness simply reverses the direction of positive quantities. If the strip is very thin, then the change in local curvature has the same response as a straight strip, otherwise, so-called through-thickness effects begin to pre-dominate during activation, and the response needs to be modified. A full treatment [10] concludes that the thickness must be, at least, an order of magnitude smaller than the local helical radius for no change in the expected behaviour, and is assumed here.

During activation, equal and opposite tensile axial forces, F, are applied to the structure, Fig. 4(a), giving way to a relative displacement, δ, between its ends in the same direction. These parameters are presumed to be concentric to ensure a uniformity of deformation around the larger helical path: the axial force could be applied physically to either end of the coiled coil by short lever arms. Even so, a formal solution of the structural behaviour for all possible initial geometries is likely to be difficult, given the geometrical complexity and the lack of closed-form solutions explicitly relating F and δ in analogous but simpler problems of ordinary coiled springs [11]. A more transparent approach, however, utilises the following assumptions based on actual coil geometries [7], and it results in relatively straightforward and separate treatments of equilibrium and compatibility. In particular, the larger helix has a much greater radius, denoted as b, than the radius, a, of the local helical path, and both helices are *closely coiled* during winding. The associated angle of inclination, or pitch, of the larger helix is practically zero and, accordingly, any small portion of the coiled coil has negligible toroidal curvature. The axis of the smaller helix can therefore be treated as being straight, and changes in curvature along the strip do not distort the radius of the larger path. From overall moment equilibrium with the applied load, Fig. 4(b), the twisting torque acting everywhere along the larger helical path is simply Fb. It is also clear from Fig. 4(b) that a vertical shear force, F, acts across the smaller helix, which is carried

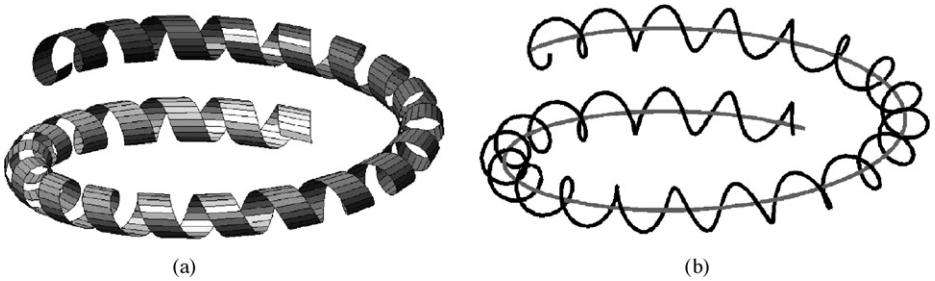

(a) (b)

Fig. 3. (a) Schematic of strip-like coiled coil; (b) distinction between the larger helical path (grey) and the smaller, localised helical path (black). In both sub-figures, both helical paths are right-handed.

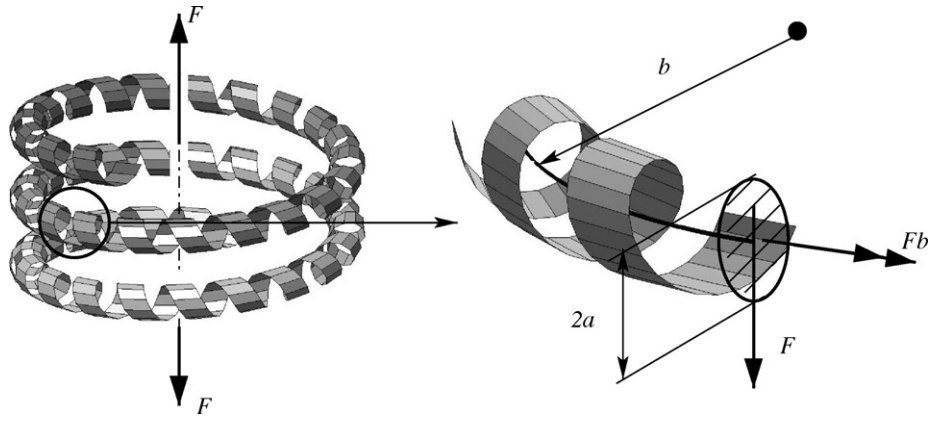

Fig. 4. Equilibrium response of a general coiled coil under axial force F. For a closeness of initial coiling, all radial planes of the smaller helical path, shaded on the right and of radius, a, approximately carry a vertical shear force, F, and a torque, Fb, where b is the larger helical radius.

by a combination of bending, twisting and shearing along the strip; for present purposes, its effect upon overall deformation is discounted although a more in-depth study is needed to reinforce this point. Denoting the smaller helix pitch angle as β, the bimorph cross-section everywhere carries the torque as a conventional bending moment, $Fb\cos\beta$, and a normal twisting torque, $Fb\sin\beta$; but under small β, the latter component is negligible, and former is approximately set to Fb, which now equates to M in Eq. (7).

The relationship between δ and κ can be solidified from the compatibility description in Fig. 5. A single turn of the larger helical path, initially flat under the close-coiled assumption, must deform uniformly into another helix by symmetry, of the same radius, b, and having a relative displacement D between its ends. For N turns, $\delta = DN$. Under pure bending activation, the arc-length of the smaller helix wrapped around this single turn is conserved: and if the angle subtended by the path increases from θ to $\theta + \Delta\theta$, where $\Delta\theta$ is a relatively small change, it can be shown that $\kappa = \Delta\theta/a\theta$. The axial displacement under $\Delta\theta$ is simply $b\Delta\theta$ and can be verified by integrating the product of equivalent twist rate, $\Delta\theta/2\pi b$ shown as ϕ in Fig. 5(b), and lever arm, b, around the turn. From simple helical geometry, θ is equal to $2\pi b/a\tan\beta$, and can be combined with the above information to yield, ultimately:

$$\kappa = \frac{\delta\beta}{2\pi b^2 N}, \tag{10}$$

and $\tan\beta \approx \beta$ for small angles. This expression is substituted in the first line of Eq. (7), along with $M = Fb$ and $V = E_3 t/2$, to produce:

$$\delta = \left[\frac{24\pi N b^3 s_{11}^E}{\beta w t^3}\right] F + \left[\frac{12\pi N b^2 d_{31}}{\beta t^2}\right] V. \tag{11}$$

Since the bending moment is uniform throughout, there is no variation in the charge density, q, so that the total charge, Q, multiplies q by the arc-length, s, of the coiled coil, $(a\theta/\cos\beta)N$ with θ defined above, and the second line of the previous matrix becomes:

$$Q = qs = \left[\frac{12\pi N b^2 d_{31}}{\beta t^2}\right] F + \left[\frac{8\pi N w e_{33}^T b}{\beta t}\left(1 - \frac{k_{31}^2}{4}\right)\right] V. \tag{12}$$

Finally, re-casting Eqs. (11) and (12) in the matrix form of Eq. (8), then its coefficients are

$$A = \frac{24\pi N s_{11}^E}{\beta w}\left(\frac{b}{t}\right)^3, \qquad B = \frac{12\pi N d_{31}}{\beta}\left(\frac{b}{t}\right)^2,$$
$$C = \frac{8\pi N w e_{33}^T}{\beta}\left[1 - \frac{k_{31}^2}{4}\right]\left(\frac{b}{t}\right). \tag{13}$$

Terms equivalent to B and to B/A are derived in [7] but by separate calculations of the freely actuated displacement and the force required to nullify, or "block", displacements; no general structural or electrical behaviour is formulated. When the small angle assumption is not relaxed, the blocking force offered here is the same as in [7]; but their B term differs slightly by virtue of being proportional to $2\pi N + \sin 2\pi N$ rather than $2\pi N$ alone. The

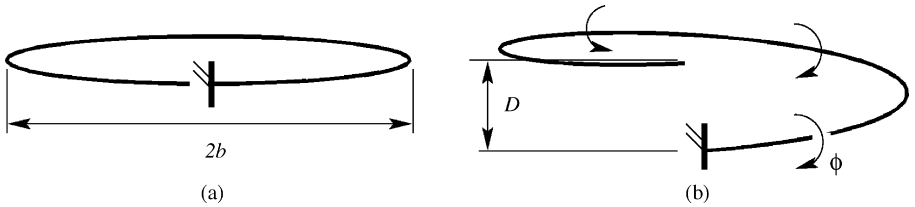

Fig. 5. Compatibility requirements for the larger helical path of coiled coil: (a) initial, flat configuration, assuming negligible pitch angle; (b) helically deformed path due to uniform twist-rate, ϕ, along the circumferential length, resulting in a vertical displacement, D, for each turn of path.

reason is due to different boundary conditions; here, the rotational symmetry of the deformed larger helical path is met by a change in slope at both ends (indeed, everywhere), but in [7], one of the ends is rigidly fixed, and the axis of the larger path must deviate during deformation, causing a sinusoidal perturbation in displacements when they are measured in the vertical direction.

Having established the electromechanical coupling behaviour, it is now possible to quantify most aspects of the device operation, and is expedited by the general matrix description in Eq. (8) and compared to the tip-loaded straight bimorph, as noted before. The following section considers two distinct features: first, the general structural response in view of the raw mechanical output, as defined by the properties imbued in the first line of Eq. (8); second, the efficiency of device, which draws on the mechanical and electrical energy performances, and must consider all matrix terms.

3. Performance and efficiency

Several performance characteristics can be defined for a mechanical actuator, and the reader is referred to [12] for more detail. They depend fundamentally upon the properties of compliance (or stiffness), freely actuated strain, and generative force, which can be interpreted from the previous matrix coefficients in a more precise way. The structural compliance is A (m/N), the freely actuated displacement is BV (m), and one measure of the generative force is the blocking force under zero displacement, and is $-BV/A$ (N). Another useful property is the natural frequency, f, which is estimated by assuming that all of the mass, m, moves in unison, as in an elementary lumped mass-spring analogy in which $f \approx \sqrt{1/Am}/2\pi$ (Hz), $1/A$ being the equivalent spring stiffness. The results are summarised below by defining ratios for each property between the coiled coil and straight strip using the coefficients from Eqs. (13) and (9), and denoting with the subscripts "cc" and "str", respectively: identical piezoelectric material properties and activation levels for both structures should also be assumed. Note that the mass is proportional to the arc-length of structure, equal to $(\pi N/\beta)2b$ for the coiled coil and to L for the straight strip:

$$\text{compliance ratio}: \quad \frac{A_{cc}}{A_{str}} = \frac{3}{4}\frac{\pi N}{\beta}\left(\frac{2b}{L}\right)^3 \tag{14a}$$

$$\text{free displacement ratio}: \quad \frac{B_{cc}}{B_{str}} = \frac{\pi N}{\beta}\left(\frac{2b}{L}\right)^2 \tag{14b}$$

$$\text{blocking force ratio}: \quad \frac{B_{cc}/A_{cc}}{B_{str}/A_{str}} = \frac{4}{3}\left(\frac{L}{2b}\right) \tag{14c}$$

$$\text{natural frequency ratio}: \quad \sqrt{\frac{A_{str}m_{str}}{A_{cc}m_{cc}}} = \frac{2}{\sqrt{3}}\frac{\beta}{\pi N}\left(\frac{L}{2b}\right)^2. \tag{14d}$$

The common terms $\pi N/\beta$ and $2b/L$ define relative geometrical features. The more straightforward latter term indicates the planar size between structures whilst the former is a "compactness" parameter, for it is strictly the arc-length of strip per unit width of the larger helical path, and typically lies in the range 10–20 for each turn of path for small β. It amplifies geometrically dependent properties, as can be seen above, such as the freely actuated displacement and the mass, as well as the ordinary elastic displacements and, hence, the compliance that, in turn, leads to a smaller natural frequency of the coiled coil. Only the blocking force ratio is independent of the number of turns, N, for the reacting bending moment is carried uniformly at the level of the small helix; and for "same size" devices, where $L = 2b$, the ratio is 4/3 in favour of the coiled coil since the bending moment in the straight strip is not uniform but increases from zero at the tip to a maximum at the root.

The electrical performance of the coiled coil is now considered in view of its efficiency, i.e. its ability to convert input energy into useful mechanical work. The enabling electromechanical coupling behaviour has one drawback in this respect, for both elastic strain energy due to the build-up of stresses and electrical energy due to the capacitative nature of the material are stored. Therefore, not all of the input energy is available for performing output mechanical work compared to conventional but ideal transducers, and the efficiency levels are expected to be small. However, the potential for output work can be extracted from contrived operational scenarios, for the sake of transparency. One historic measure defines the ratio of mechanical energy stored in a strip relative to the electrical energy input under uniform clamping conditions, in which axial strains are prevented during application of an open-circuit electric field, which draws no current; and from Mason [1], this ratio has the value of $d_{31}^2/s_{11}e_{33}^T$, denoted as k_{31}^2, cf. Eq. (5). This parameter is quoted by piezoelectric manufacturers as one of the fundamental coupling coefficients, for the uniformity of deformation ensures a maximum interchange of energies; for the highest available value of k_{31} of about 0.44 [3], the best response is approximately 20%. The final state can be reached by allowing the strip to expand freely under the electric field, which is held constant, and then restoring the axial extension to zero by application of an axial force; components of stored energy are acquired *sequentially*, which shortens their analytical determination. The response of a coiled coil (and straight strip) can be pursued under similar clamping conditions. The presentation follows from [2] and is again normalised by the use of the previous matrix coefficients: the blocking force and freely actuated displacements in the following are denoted by F_0 and δ_0, respectively.

The electrical work performed by the source in transferring a charge, Q, at voltage V to the bimorph is $0.5QV$ from elementary physics. Upon substituting for Eq. (8), the electrical energy, U_{elect}, directed into moving the displacement to δ_0 is

$$U_{elect} = \tfrac{1}{2}[BF + CV]V. \tag{15}$$

Since the external force is zero, $U_{elect} = 0.5CV^2$, and the actuator behaves, electrically, as a pure capacitor. No current is drawn from it and the total charge and U_{elect} remain invariant. A force is then applied to restore the original extension to zero, and the

elastic energy now stored in the device is calculated from

$$U_{\text{elastic}} = \int_{\delta_0}^{0} F \, \mathrm{d}\delta, \tag{16}$$

where

$$F = \frac{1}{A}[\delta - BV], \tag{17}$$

from the first line of Eq. (8). Inserting into Eq. (16) and performing the integration:

$$U_{\text{elastic}} = \frac{1}{2}\frac{B^2}{A}V^2 = -\frac{1}{2}F_0\delta_0, \tag{18}$$

which is the magnitude of the area under the graph of F versus δ between zero and δ_0, and the elastic strain energy gained by the device is equal to the work done by the external force. Returning to the form in Eq. (18), an electromechanical coupling coefficient for the device, k^2, can be defined as

$$k^2 = \frac{U_{\text{elastic}}}{U_{\text{elect}}} = \frac{1/2(B^2/A)V^2}{1/2(CV^2)} = \frac{B^2}{CA}, \tag{19}$$

and substituting for the terms A, B and C with Eqs. (13) and (9), the respective expressions for a coiled coil and straight strip are

$$k_{\text{cc}}^2 = \frac{3}{4}\frac{k_{31}^2}{[1-(k_{31}^2/4)]}, \tag{20a}$$

$$k_{\text{str}}^2 = \frac{9}{16}\frac{k_{31}^2}{[1-(k_{31}^2/4)]}. \tag{20b}$$

Note that both ratios do not contain any geometric terms. The 33% increase in value offered by the coiled coil is due solely to the uniform bending moment everywhere and optimal distribution of the elastic strain energy cf. the same increase in the previous blocking force ratio. In addition, k^2 can never be greater than the maximum efficiency of the piezoelectric material: indeed, for a coiled coil, the largest difference between efficiencies occurs when $k_{31}^2 = 4 - 2\sqrt{3} = 0.536$ with $k_{\text{cc}}^2 = 0.464$. For a maximum practical value of $k_{31} = 0.44$, k_{cc}^2 is equal to 0.16.

While k_{cc}^2 provides a useful comparison to the fundamental coefficient, k_{31}^2 it is a rather hypothetical measure for no mechanical output work is performed under the clamped conditions. Instead, consider a second case of an "unclamped" coiled coil that performs work against an external but constant force. It is possible to define an energy transmission coefficient, λ, concomitant with the actual output work relative to the input electrical energy [13]. If the final displacement of the coiled coil is δ, the work done is $-F\delta$, where it is assumed that F is negative as obviated by the need for positive effort. Replacing δ with Eq. (8) and using Eq. (15), λ may be expressed as

$$\lambda = \frac{\text{output work}}{U_{\text{elect}}} = \frac{[AF + BV]F}{0.5[BF + CV]V}. \tag{21}$$

For known values of F and V, λ may be found, e.g. if the applied force is one half of the blocking force, $F = -BV/2A$, then:

$$\lambda = \frac{[B^2/2AC]V^2}{[1-(B^2/2AC)]V^2} = \frac{k^2}{2-k^2}, \tag{22}$$

using Eq. (19), and is about 8.7% at best for a coiled coil using Eq. (20a). Of specific interest, is the combination of F and V that gives rise to maximum λ, as performed in [3]. Dividing the top and bottom lines of Eq. (21) by V^2 and denoting F/V as x:

$$\lambda = -\frac{2[Ax^2 + Bx]}{Bx + C}. \tag{23}$$

Differentiating λ with respect to x, and setting equal to zero, forces a pair of negative roots:

$$x = -\frac{C}{B} \pm \left[\frac{C^2}{B^2} - \frac{C}{A}\right]^{0.5} \tag{24}$$

Inserting the smallest root back into Eq. (23) and using Eq. (19):

$$\lambda_{\text{max}} = \frac{2}{k^2}[2 - k^2 - 2(1-k^2)^{0.5}], \tag{25}$$

which can be re-written as

$$\lambda_{\text{max}} = 2\left[\frac{1}{k^2} + \left[\frac{1}{k^2} - 1\right] - 2\left[\frac{1}{k^2}\left(\frac{1}{k^2} - 1\right)\right]^{0.5}\right]$$
$$= 2\left[\left(\frac{1}{k^2}\right)^{0.5} - \left(\frac{1}{k^2} - 1\right)^{0.5}\right]^2. \tag{26}$$

Substituting for k_{cc}^2 and k_{str}^2 from Eqs. (20a) and (20b), and re-arranging:

$$\lambda_{\text{max,cc}} = \frac{8}{3k_{31}^2}\left[\left(1 - \frac{k_{31}^2}{4}\right)^{0.5} - (1-k_{31}^2)^{0.5}\right]^2, \tag{27a}$$

$$\lambda_{\text{max,str}} = \frac{32}{9k_{31}^2}\left[\left(1 - \frac{k_{31}^2}{4}\right)^{0.5} - \left(1 - \frac{13k_{31}^2}{16}\right)^{0.5}\right]^2. \tag{27b}$$

Again, the results do not contain geometric parameters and they are compared in Fig. 6 up to the practical limit of $k_{31} = 0.44$. As

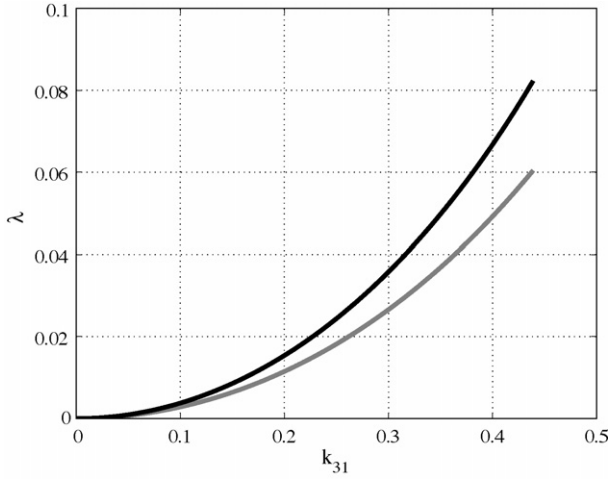

Fig. 6. Comparison of energy transmission coefficients, λ, between a coiled coil (black) and a straight bimorph (grey). The coefficients measure the ability to convert electrical input energy into useful mechanical work against a constant resistive force, and k_{31}^2 is a fundamental material coupling coefficient, which has a maximum value of 0.44^2.

expected, the coiled coil fairs better, transmitting approximately 36% more energy at maximum conditions over the straight bimorph, but only managing a total transfer of around 10% of the input electrical energy. The corresponding F/V ratios are given by Eq. (24) and, after some manipulation, it can be shown that:

$$\frac{(F/V)_{\max,cc}}{(F/V)_{\max,str}} = \left(\frac{L}{2b}\right)\left[\frac{\lambda_{\max,cc}k_{cc}^2}{\lambda_{\max,str}k_{str}^2}\right]^{0.5}, \quad (28)$$

which has a maximum value of 1.348 when $k_{31} = 0.44$, if L is set equal to $2b$: the force generated by a coiled coil under maximum energy transfer conditions is approximately 35% more than the equivalent force for a straight strip of the same size under the same levels of activation.

4. Conclusions

From an actuation viewpoint, the localised helical curving of a piezoelectric coiled coil bimorph strip offers two complementary features: the amplification of activated bending strains into substantial axial displacements and the development of a uniform bending moment everywhere along the strip under an axial force for an optimal structural behaviour. Compared to a commercially available straight tip-loaded strip, which is not uniformly stressed, the coiled coil generates 33% more blocking force, and is 36% more energetically efficient when the structures are approximately the same size; freely actuated displacements increase tenfold and more. The coiled coil has a much lower axial stiffness and, due to the substantial arc-length embraced by the overall device, its mass also increases disproportionately and the natural frequency is, at least, an order magnitude less—from the properties given in [7], absolute values are calculated approximately to be around 50–100 Hz. In [12], the ceiling of any forced frequency operation is recommended to be the natural frequency, otherwise power is consumed thereafter as the inverse square of the driving frequency and there is risk of material breakage as displacements are exacerbated at resonance. For these reasons, the coiled coil dynamical performance has not been detailed, and it is suggested that its operation is limited to low-frequency applications that demand relatively large changes in shape.

Acknowledgments

Comments from two anonymous reviewers were cordially received.

References

[1] W.P. Mason, Piezoelectric crystals and their applications to ultrasonics, Van Nostrand, New York, 1950.
[2] J.G. Smits, T.K. Cooney, The effectiveness of piezoelectric bimorph actuator to perform mechanical work under various constant loading conditions, Ferroelectrics 119 (1–4) (1991) 89–105.
[3] Q.M. Wang, X.H. Du, L.E. Cross, Electromechanical coupling and output efficiency of piezoelectric bending actuators, IEEE Trans. Ultrason. Ferroelectr. Freq. Control 46 (3) (1999) 638–646.
[4] D.H. Pearce, Piezoelectrics spring into action, Mater. World 7 (12) (1999) 748–750.
[5] F. Mohammadi, A.L. Kholkin, D. Jadidian, A. Safari, High-displacement spiral piezoelectric actuators, Appl. Phys. Lett. 75 (16) (1999) 2488–2490.
[6] D.H. Pearce, K.A. Seffen, T.W. Button, Net shape formed spiral and helical piezoelectric actuators, J. Mater. Sci. 37 (2002) 3117–3122.
[7] D.H. Pearce, A. Hooley, T.W. Button, On piezoelectric super-helix actuators, Sens. Actuators A: Phys. 100 (2002) 281–286.
[8] P.X. Gao, Y. Ding, W. Mai, W.L. Hughes, C. Lao, Z.L. Wang, Conversion of zinc oxide nanobelts into superlattice-structured nanohelices, Science 309 (2005) 1700–1704.
[9] S.K. Ha, Analysis of the asymmetric triple-layered piezoelectric bimorph using equivalent circuit models, J. Acoust. Soc. Am. 110 (2) (2001) 856–864.
[10] K.A. Seffen. Through-thickness effects in curved piezoelectric beams. Technical report, Department of Applied Mechanics, UMIST, Manchester: UMIST/ME/AM/14.05.01/CURV1, 2001.
[11] J.W. Phillips, G.A. Costello, Large deflections of impacted helical springs, J. Acoust. Soc. Am. 51 (2) (1972) 967–973.
[12] J.E. Huber, N.A. Fleck, M.F. Ashby, The selection of mechanical actuators based on performance indices, Proc. R. Soc. Lond. A 453 (1997) 2185–2205.
[13] K. Uchino, Piezoelectric Actuator and Ultrasonic Motors, Kluwer Academic, Boston, MA, 1996.

Biography

Keith Seffen holds MA (1997) and PhD (1997) degrees from the University of Cambridge. His postgraduate research dealt with deployable spacecraft structures; as a post-doctoral scientist, he pursued topics in configuration optimisation before being appointed to lectureship in Smart Structures and Materials at UMIST, UK, where he developed interests in solid-state actuators, in collaboration with academic partners on a European Union funded project (G1RD CT 1999 0121). He is currently a lecturer in the Structures Group at Cambridge University Engineering Department, where he founded the Laboratory for Reconfigurable Structures Research (http://www2.eng.cam.ac.uk/~kas14/research.html). He is a member of the American Institute of Aeronautics and Astronautics (AIAA) and the Institute of Maths and its Applications (IMA).